Journal of Contaminant Hydrology 116 (2010) 58–72

Contents lists available at ScienceDirect

Journal of Contaminant Hydrology

journal homepage: www.elsevier.com/locate/jconhyd

Influence of adsorption on phenol transport through soil–bentonite vertical barriers amended with activated carbon

Michael A. Malusis [a,*], James E. Maneval [b,1], Edward J. Barben [c,2], Charles D. Shackelford [d,3], Emily R. Daniels [a,4]

[a] Department of Civil and Environmental Engineering, Bucknell University, Lewisburg, PA 17837, USA
[b] Department of Chemical Engineering, Bucknell University, Lewisburg, PA 17837, USA
[c] Gannett Fleming, Inc., 207 Senate Avenue, Camp Hill, PA 17011, USA
[d] Department of Civil and Environmental Engineering, Colorado State University, 1372 Campus Delivery, Fort Collins, CO 80523, USA

ARTICLE INFO

Article history:
Received 11 January 2010
Received in revised form 29 May 2010
Accepted 1 June 2010
Available online 9 June 2010

Keywords:
Activated carbon
Cutoff wall
Nonlinear adsorption
Phenol
Retardation
Soil–bentonite vertical barrier

ABSTRACT

The potential for enhanced containment of phenol by soil–bentonite (SB) vertical barriers amended with activated carbon (AC) was investigated. Results of batch equilibrium adsorption tests on model SB backfills amended with 0–10 wt.% granular AC (GAC) or powdered AC (PAC) illustrate that the backfills exhibited nonlinear adsorption behavior that was described well by both the Freundlich and Tóth adsorption models. The AC amended backfills exhibited enhanced phenol adsorption relative to unamended backfill due to hydrophobic partitioning to the AC. Adsorption capacity increased with increasing AC content but was insensitive to AC type (GAC versus PAC). Results of numerical transport simulations based on the measured adsorption behavior show that the Tóth model yielded similar or lower phenol breakthrough times than the Freundlich model for the range of source concentrations (C_o) considered in the simulations (0.1–10 mg/L). Breakthrough time decreased with increasing C_o but increased with increasing AC content. Predicted breakthrough times for an SB vertical barrier amended with 2–10 wt.% AC increased by several orders of magnitude relative to the theoretical case of a nonreactive (non-adsorbing) barrier. The findings suggest that AC may be a highly effective adsorption amendment for sustaining the containment performance of SB vertical barriers.

1. Introduction

Vertical cutoff walls are widely employed as *in situ* containment barriers for isolating contaminated groundwater from the surrounding environment. The most common type of vertical barrier used in the U.S. is the soil–bentonite (SB) slurry trench cutoff wall that is named after the nature of the final barrier materials (soil–bentonite) and the method of construction (slurry trench). The typical construction process involves excavating a 0.6- to 1.2-m-wide trench to a low permeability stratum while simultaneously filling the trench with bentonite–water slurry to maintain stability (Sharma and Reddy, 2004). Trench spoils and/or imported materials are combined with desirable amendments (e.g., dry bentonite) and bentonite–water slurry to create a homogeneous, high-slump (i.e., 100 to 150 mm) mixture that subsequently is backfilled into the trench to complete the barrier (Xanthakos, 1979; D'Appolonia, 1980; Spooner, 1984; Ryan, 1987; Millet et al., 1992; Evans, 1994; Rumer and Ryan, 1995).

* Corresponding author. Tel.: +1 570 577 1683; fax: +1 570 577 3415.
E-mail addresses: michael.malusis@bucknell.edu (M.A. Malusis), maneval@bucknell.edu (J.E. Maneval), ebarben@gfnet.com (E.J. Barben), shackel@engr.colostate.edu (C.D. Shackelford), erd008@bucknell.edu (E.R. Daniels).
[1] Tel.: +1 570 577 1669.
[2] Tel.: +1 717 763 7211.
[3] Tel.: +1 970 491 5051.
[4] Tel.: +1 570 577 1112.

0169-7722/$ – see front matter © 2010 Elsevier B.V. All rights reserved.
doi:10.1016/j.jconhyd.2010.06.001

Conventional design of SB backfill is predicated upon achieving a low backfill hydraulic conductivity, k ($\leq 10^{-8}$ m/s), to inhibit groundwater flow and advective contaminant transport. However, given the significant, if not dominant, role of diffusive transport through low-k barriers (e.g., Shackelford and Daniel, 1991; Rowe et al., 1995; Khandelwal and Rabideau, 2000; Neville and Andrews, 2006), low k may not be sufficient to ensure that an SB barrier will provide effective containment over a long time span (e.g., decades). The detrimental impact of diffusive transport on the long-term effectiveness of a vertical barrier typically is mitigated through hydraulic control. For example, the conventional practice of pumping from within a circumferential cutoff wall configuration often is performed to maintain an inward hydraulic gradient, thereby actively reducing the outward flux of contaminants (e.g., see LaGrega et al., 2001). The disadvantage of this practice is the cost associated with continuous operation of the pumping system and *ex-situ* treatment of the extracted groundwater.

Recently, contaminant adsorption has been studied as a potentially significant mechanism for passively delaying the detrimental influence of diffusion through SB barriers (e.g., Khandelwal et al., 1998; Khandelwal and Rabideau, 2000; Prince et al., 2000; Gullick and Weber, 2001; Krol and Rowe, 2004). However, conventional SB barriers typically do not contain an appreciable amount of organic carbon and, thus, may exhibit limited intrinsic adsorption capacity for organic solutes such as volatile organic compounds (VOCs) (Gullick, 1998; Khandelwal et al., 1998; Krol and Rowe, 2004). As a result, high-carbon amendments such as organically modified clays (organoclays), fly ash, shale, shredded tires and activated carbon have been considered as barrier amendments to enhance VOC adsorption (e.g., Mott and Weber, 1992; Bierck and Chang, 1994; Smith and Jaffe, 1994; Gullick et al., 1996; Park et al., 1997; Lo, 2001; Gullick and Weber, 2001; Bartelt-Hunt et al., 2005). In particular, activated carbon (AC) appears to be a promising VOC adsorption amendment for SB vertical barriers in that AC generally exhibits superior VOC adsorption relative to the other amendments listed above (e.g., Bartelt-Hunt et al., 2005; Lake and Rowe, 2005). Also, several studies have shown that AC amendment may be performed without causing an adverse impact on barrier hydraulic conductivity (Bierck and Chang 1994; Bartelt-Hunt et al., 2005; Malusis and Scalia, 2007; Malusis et al., 2009).

Although VOC adsorption by pure AC has been studied extensively (e.g., Peel and Benedek, 1980; Kong and DiGiano, 1986; Chiang et al., 2001; Chern and Chien, 2002; Chuang et al., 2003; Bartelt-Hunt et al., 2005), the VOC adsorption characteristics of an SB backfill matrix containing AC has received little attention. However, Bierck and Chang (1994) reported significant retardation of 2-propanone in a column test on SB backfill amended with 2 wt.% granular AC. These limited findings suggest that additional investigation is warranted to characterize the VOC adsorption behavior of AC-amended SB backfill, to investigate the role of AC type and percentage on adsorption behavior of the backfill, and to evaluate the benefit of enhanced VOC adsorption in terms of improved containment performance of SB vertical barriers. As a first step in such an investigation, the objectives of this study were (1) to investigate the influence of AC amendment on adsorption of a selected VOC (phenol) by a model SB backfill, and (2) to assess the containment performance of an AC-amended SB cutoff wall based on the experimental findings. The impact of different percentages of a granular AC (GAC) and a powdered AC (PAC) on the phenol adsorption characteristics of the model backfill was assessed, and the potential benefit of AC amendment for phenol attenuation in representative field SB cutoff wall installations was evaluated by conducting one-dimensional contaminant transport simulations that accounted for the adsorption behavior exhibited by the AC-amended backfill mixtures.

2. Materials and methods

2.1. Solid materials

The solid materials used to prepare the model SB backfill mixtures included clean sand, powdered sodium bentonite, and two AC products. The sand was provided by Central Builders Supply (Lewisburg, PA) and was chosen to represent construction of a SB cutoff wall in a clean sand aquifer. The bentonite is commercially available under the trade name Naturalgel® (Wyo-Ben, Inc., Billings, MT) and is commonly used in SB cutoff wall applications. The bentonite was added to the backfill mixtures both as a dry amendment and via bentonite–water slurry. The AC products included: (1) bituminous GAC (size 0.297–0.074 mm; Fisher Scientific, Fair Lawn, NJ) primarily used for decolorizing oils, colored solutions and syrups; and (2) bituminous PAC (size 0.149–0.044 mm; Calgon Corporation, Pittsburgh, PA) commonly used for potable water treatment.

Measured grain-size distributions (ASTM D422-02) and soil classifications for each solid material are presented by Malusis et al. (2009). Atterberg limits (ASTM D4318-05) also were measured and are listed along with selected physical and chemical properties in Table 1. Based on the Unified Soil Classification System (ASTM D2487-00), both the sand and GAC classified as poorly graded sand (SP), whereas the PAC classified as an elastic silt (MH) and the bentonite classified as a high-plasticity clay (CH). The bentonite contained approximately 70% montmorillonite based on X-ray diffraction analysis, and the measured cation exchange capacity, *CEC*, of 83.4 $cmol_c$/kg was satisfied primarily by sodium cations (~85% of *CEC*). The total organic carbon (*TOC*) contents of the sand and bentonite were 0.13% and 0.36%, respectively, whereas the *TOC* contents of the GAC and PAC were 97.3% and 90.9%, respectively. As shown in Table 1, the GAC exhibited a lower external specific surface but a higher internal (micropore) specific surface relative to the PAC, such that the total specific surfaces (i.e., external plus internal) of the GAC and PAC were similar (i.e., 1166 m^2/g and 1140 m^2/g, respectively).

2.2. Phenol

Phenol (C_6H_5OH; Mol. Wt. = 94.1 g/mol, Certified ACS grade crystals, Fisher Scientific, Fair Lawn, NJ) was chosen as the organic solute of interest in this study. Phenol is an aromatic hydrocarbon that is ranked #182 on the 2007 CERCLA Priority List given by the Agency for Toxic Substances and Disease Registry (www.atsdr.cdc.gov/cercla/07list.html). The relatively high solubility, S_o (= 82,000 mg/L at 20 °C), low octanol–water

Table 1
Measured physical and chemical properties of solid materials used in study.

Property	Standard	Bentonite	Sand	GAC	PAC
Liquid limit, *LL* (%)	ASTM D 4218-05	488	NP	NP	113
Plasticity index, *PI* (%)	ASTM D 4218-05	443	NP	NP	5.6
Fines content (%)	ASTM D 422-02	93	<5	5.2	99
Mean particle size, d_{50} (mm)	ASTM D 422-02	--	0.20	0.16	0.019
Total organic carbon, *TOC* (%)	[a]	0.36	0.13	97	91
pH	ASTM D 4972-01	9.1	6.4	8.6	7.6
Cation exchange capacity, *CEC* ($cmol_c/kg$)	[b]	83.4	–	–	–
Specific surface (m^2/g)					
External	[c]	–	–	96	233
Micropore				1070	907
Total				1166	1140
Principal minerals (%)					
Montmorillonite	[d]	69	–	–	–
Cristobalite		14			
Quartz		12			
Other		5			

GAC = granular activated carbon; PAC = powdered activated carbon; NP = non-plastic.
[a] *TOC* for bentonite and sand determined using solids *TOC* analyzer; *TOC* for GAC and PAC determined by loss on ignition.
[b] Procedures described by Shackelford and Redmond (1995).
[c] Results of multipoint BET (external) and t-method (micropore) analyses performed by Quantachrome Instruments (Boynton Beach, FL).
[d] Results of X-ray diffraction analyses performed by Mineralogy Inc. (Tulsa, OK).

partition coefficient, K_{ow} (=28.8), and low organic carbon partition coefficient, K_{oc} (=14.2 mL/g), of phenol suggest that phenol is more hydrophilic than many common VOC pollutants, such as benzene (S_o=1780 mg/L at 25 °C, K_{ow}=132, K_{oc}=83.0 mL/g), toluene (S_o=515 mg/L at 20 °C, K_{ow}=537, K_{oc}=300 mL/g) and trichloroethene (S_o=1100 mg/L at 25 °C, K_{ow}=240, K_{oc}=126 mL/g) (see LaGrega et al., 2001). In this respect, phenol may be considered as a conservative surrogate compound for use in examining the benefits of AC amendment on VOC containment performance of SB cutoff walls.

2.3. Slurry and backfill preparation

Bentonite–water slurry (5% bentonite by mass) was prepared by blending the bentonite with tap water (pH=6.91; electrical conductivity, EC=14.3 mS/m) in a high-shear mixer (i.e., a Hamilton Beach 7-speed blender at the highest setting) for 5 min. The slurry was allowed to hydrate for a minimum of 24 h prior to use. After hydration, the measured mud density and Marsh cone viscosity of the slurry were 1.033 g/cm^3 and 38 s, respectively. The model SB backfills then were prepared by combining the sand, dry bentonite, GAC or PAC, and slurry in a Hobart mixer (Model #N50, Hobart Corp., Troy, OH) to ensure uniformity. Slurry was added incrementally until a target slump of 125 ± 12.5 mm was achieved in triplicate using a standard slump cone (ASTM C143-00). The total bentonite content (dry bentonite plus bentonite from slurry) in all of the backfill mixtures was held constant at 5.8 wt.% to facilitate comparison of test results. Additional details regarding backfill preparation are provided in Barben et al. (2008). Relevant properties of each backfill mixture are presented in Table 2.

2.4. Adsorption testing

Adsorption isotherms for each backfill mixture were measured using batch equilibrium adsorption tests adapted from guidelines given by Roy et al. (1992). Phenol solutions were prepared by mixing the phenol with distilled water (pH=6.82, EC=0.44 mS/m). The solid materials and water used to prepare the backfills and phenol solutions were autoclaved to minimize the potential for biodegradation of phenol during the tests. Backfill samples of known mass were placed into 40-mL amber EPA vials (Fisher Scientific, Fair Lawn, NJ), and the vials were filled with phenol solutions of varying source concentrations (C_o) to achieve a solid:solution ratio, or SSR (ratio of dry mass of solids to volume of solution), of 1:10. To minimize volatility losses, the vials were completely filled (i.e., no headspace) and topped with Teflon-lined caps. The vials were tumbled end-over-end for a period of 72 ± 2 h in an aluminum tumbler box. The 72-h period was determined from preliminary adsorption experiments to be sufficient for achieving equilibrium conditions. After tumbling, supernatant removed from each vial was centrifuged at 800 *g* for 15 min at 20 °C and then filtered through a 0.45-μm PTFE syringe filter (Cole-Parmer, Vernon Hills, IL) via a 2.5-mL GASTIGHT® syringe (Hamilton Company, Reno, NV). The filtered centrate was transferred directly into an autosampler vial lined with a 0.25-mL glass conical insert (Supelco, St. Louis, MO).

The equilibrium phenol concentration (C_e) in the filtered centrate was measured using an Ultimate 3000 high-performance liquid chromatograph (HPLC) with UV–Visible detector (Dionex Corp., Sunnyvale, CA). The HPLC operating parameters for phenol included an eluent of 59% methanol (Optima grade, Fisher Scientific) and 41% deionized water, an eluent flow rate of 1.0 mL/min, a detection wavelength of 218 nm, and an injection volume of 100 μL. The phenol detection limit associated with these conditions was determined to be approximately 10 μg/L. Each backfill was subjected to triplicate testing (i.e., three replicate vials) at each source concentration. Spike vials containing the source

Table 2
Relevant properties of model soil–bentonite backfill mixtures (total bentonite content in all mixtures = 5.8% by dry wt).

Backfill No.	AC content (%)	AC type	*TOC* content (%)	Fines content (%)	Gravimetric water content (%)	Mean slump (mm)	Paste *pH*
1	0	–	0.14	10.5	43.3	128	8.68
2	2	GAC	2.09	10.5	43.5	128	8.62
3	5	GAC	5.00	10.5	46.3	127	8.81
4	10	GAC	9.85	10.5	52.1	123	8.53
5	2	PAC	1.96	12.4	44.9	119	8.61
6	5	PAC	4.68	15.3	48.3	121	8.45
7	10	PAC	9.22	20.0	53.1	131	8.29

AC = activated carbon; GAC = granular activated carbon; PAC = powdered activated carbon; *TOC* = total organic carbon.

phenol solutions and no solids were subjected to the same procedure and confirmed that losses due to volatilization or sorption to glassware were insignificant.

3. Results and discussion

3.1. Adsorption tests

Measured adsorption data for each backfill mixture are displayed graphically in Fig. 1. The data are plotted on a semi-logarithmic scale in Fig. 1 for ease of comparing the adsorption behavior of the different backfills. Each data point represents one measurement of adsorbed (solid) phenol concentration (C_s) plotted against the corresponding C_e. The data were obtained using a wide range of source phenol concentrations ($50 \le C_o \le 1000$ mg/L) in order to define the trends in C_s over a wide range of C_e.

The results in Fig. 1 indicate that the phenol adsorption behavior of the backfill mixtures is highly nonlinear, as reflected by the steep slope of the data trends at low C_e and the concavity of the data as C_e increases. As expected, the AC-amended backfills exhibit substantially greater phenol adsorption capacity than the control backfill (0% AC). The maximum C_s values measured for the AC-amended backfills ranged from 3700 to 10,000 mg/kg (depending on the AC content), whereas the highest C_s for the control backfill was approximately 150 mg/kg.

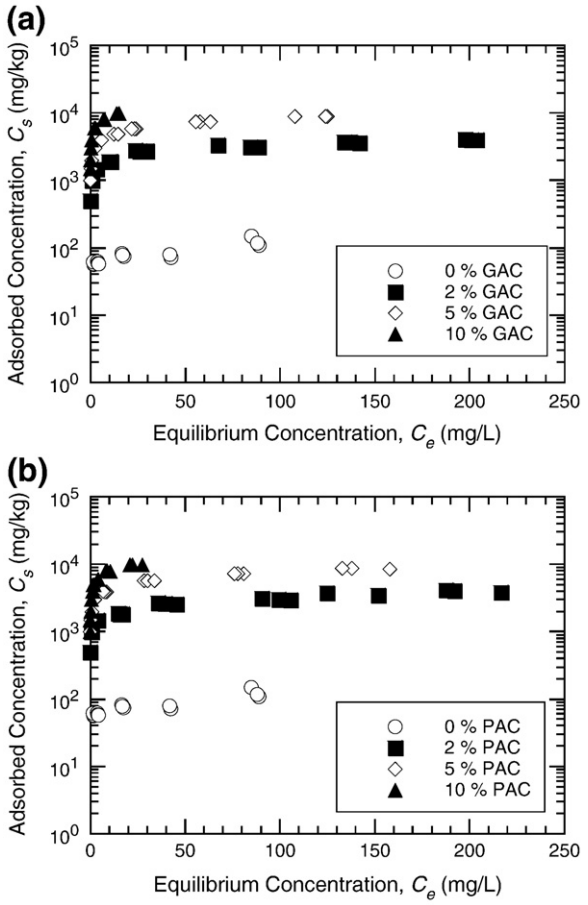

Fig. 1. Measured phenol adsorption data for backfills amended with (a) granular activated carbon (GAC) and (b) powdered activated carbon (PAC).

Phenol retention by the control backfill, although low in comparison to the AC amended backfills, was stronger and more nonlinear than observed for other organic solutes in similar studies on bentonite and SB mixtures. For example, Gullick (1998) observed that adsorption of trichloroethene (TCE) and trichlorobenzene to bentonite was negligible. Khandelwal et al. (1998) and Krol and Rowe (2004) observed that adsorption of TCE to SB mixtures containing 2% to 6% bentonite was approximately linear, with modest distribution coefficients, K_d, ranging from 0.2 to 0.7 L/kg. Given the low organic carbon content of the control backfill used in this study (see Table 2), the observed phenol adsorption by the control backfill may be attributed to irreversible interactions between the phenol and the bentonite rather than hydrophobic partitioning. For example, similar behavior was observed in bentonite-phenol adsorption tests conducted by Banat et al. (2000), who reported phenol adsorption capacities of 433, 842, and 1712 mg/kg corresponding to solution *pH* values of 11, 8, and 5, respectively. Banat et al. (2000) attributed the phenol retention largely to irreversible processes of hydrogen bonding and/or adsorption to the bentonite through charge transfer complexes, noting that the decrease in measured adsorption capacity with increasing *pH* is due to greater ionization of phenol (a weak acid with $pK_a = 10$) into phenolate anions ($C_6H_5O^-$) that tend to be repelled by the negatively charged bentonite particle surfaces. Measured *pH* values of the filtered centrate in the test conducted on the control backfill ranged from 9.0 to 9.3. Therefore, the appreciable phenol retention exhibited by the control backfill in Fig. 1 is consistent with the observations made by Banat et al. (2000).

Three nonlinear adsorption models were used to fit the adsorption data in Fig. 1, viz., (1) the Langmuir model, (2) the Tóth model, and (3) the Freundlich model. The Langmuir model is founded on the assumption that adsorption occurs at energetically homogeneous sites within the adsorbent (e.g., Harmsen, 1982). The resulting model expression is given as follows:

$$C_s = \frac{Q_L K_L C_e}{1 + K_L C_e} \tag{1}$$

where K_L is the Langmuir constant representing the binding strength of the adsorption sites for the solute and Q_L is the maximum adsorbed concentration (i.e., adsorption capacity) of the solute. In contrast, the Tóth model assumes a heterogeneous distribution of adsorption energy across the adsorbent surface (Allen et al., 2004) and, therefore, can be expressed as follows (Hinz, 2001):

$$C_s = \frac{Q_T K_T C_e}{\left[1 + (K_T C_e)^{N_T}\right]^{1/N_T}} \tag{2}$$

where K_T and Q_T are analogous to the Langmuir parameters (K_L and Q_L) and N_T is an exponent that represents the degree of heterogeneity associated with the adsorption. For

homogenous adsorption, $N_T = 1$ and Eq. (2) reduces to the Langmuir model (Eq. (1)). The Freundlich model is an empirical power function given as follows:

$$C_s = K_F C_e^{N_F} \quad (3)$$

where K_F is the Freundlich unit adsorption capacity. The Freundlich exponent, N_F, in Eq. (3) is considered a joint measure of the relative magnitude and diversity of adsorption energies (Weber et al., 1992) and is less than unity (i.e., $N_F < 1$) for concave, nonlinear adsorption.

The Langmuir and Freundlich models are commonly used to fit nonlinear adsorption data for soil (Kinniburgh, 1986; Limousin et al., 2007) and have been incorporated into several commercially-available transport codes for simulating the migration of contaminants in groundwater systems and soil barriers (e.g., Srinivasan and Mercer, 1987; Rowe et al., 1994; Zheng and Wang, 1999). In addition, both models were considered by Banat et al. (2000) to be applicable for describing nonlinear adsorption of phenol to bentonite. The Tóth model, originally developed for adsorption of vapors, is less commonly applied to soil systems, but has proven to be useful for describing adsorption of organic solutes, including phenolic compounds, onto activated carbon and other carbon-rich materials (e.g., Ho et al., 2002; Terzyk et al., 2003; Wu et al., 2004).

Best-fit values of the Langmuir, Freundlich, and Tóth parameters were obtained by nonlinear (unweighted), least squares regression of the isotherms, following the recommendation by Kinniburgh (1986). The regression procedure is an iterative approach based on the Levenberg–Marquardt algorithm that minimizes the sum of the squared error between the experimental data and the fitted model. The best-fit parameters and corresponding standard errors are summarized along with the coefficients of determination (R^2) for each regression in Table 3. Also, the regressions are plotted against the measured data for the control backfill (0% AC) in Fig. 2 and the AC-amended backfills in Fig. 3. The results indicate that the Freundlich and Tóth models provide better fits to the experimental data (i.e., higher R^2 values) relative to the Langmuir model in all cases, although none of the models fit the data for control backfill particularly well (see Fig. 2). The more erratic adsorption behavior of the control backfill may be due to irreversible interactions between phenol and the bentonite fraction, as previously described. The results in Fig. 3 show that the Freundlich and Tóth models provide excellent fits to the experimental data for the AC-amended backfills. Moreover, the Freundlich and Tóth models provide closer fits to the adsorption data at low C_e (<5 mg/L) than the Langmuir model. Accurate depiction of adsorption at low C_e is important for field applications in which VOC concentrations in groundwater typically are on the order of a few mg/L or lower.

Best-fit values of the Freundlich unit capacity, K_F, and the Freundlich exponent, N_F, are plotted as a function of AC content in Fig. 4a and Fig. 4b, respectively. The K_F values in Fig. 4a increase linearly over nearly two orders of magnitude with increasing AC content, from 44.5 L/kg (0% AC) to 4317 L/kg (10% GAC) and 3726 L/kg (10% PAC). The increase in K_F with increasing AC content is statistically significant, given the relatively low standard errors (<5% in most cases) associated with these parameters (see Table 3). Values of K_F for GAC-amended backfills are ~13% higher, on average, than K_F values for backfills amended with the same percentage of PAC, which could be due to the ~18% greater internal surface area of the GAC relative to the PAC (see Table 1). As noted by Heilshorn (1991), the internal surface surrounds VOC molecules within the cavernous micropores, thereby creating favorable conditions for VOC adsorption. The N_F values in Fig. 4b range from 0.207 to 0.312, representing significant deviations from linear adsorption characterized by $N_F = 1$.

The fitted adsorption capacities based on the Tóth model (Q_T) also increase with increasing AC content, as expected (see Fig. 4c). However, the standard errors associated with the estimates of Q_T are large (31% to 97%; see Table 3). According to Kinniburgh (1986), large standard errors may be expected when fitting a three-parameter model to a limited number of data points. In addition, the results in Fig. 3 indicate that the true adsorption capacities had not been

Table 3
Summary of best-fit Freundlich, Langmuir, and Tóth model parameters for phenol adsorption to SB backfill mixtures (solid:solution ratio = 1:10).

Mix ID	Freundlich model [a]			Langmuir model [a]			Tóth model [a]			
	K_F (L/kg)	N_F	R^2	K_L (L/mg)	Q_L (mg/kg)	R^2	K_T (L/mg)	Q_T (mg/kg)	N_T	R^2
0% AC	44.5	0.207	0.830	0.464	101.3	0.680	643.1	364.1	0.149	0.809
	(13.0)	(17.4)		(42.2)	(8.59)		(162)	(31.1)	(18.3)	
2% GAC	1071	0.249	0.987	0.141	3700	0.930	163.5	18386	0.138	0.990
	(3.83)	(3.61)		(18.4)	(3.65)		(226)	(57.0)	(27.9)	
2% PAC	937	0.269	0.982	0.0982	3667	0.871	36.50	15810	0.156	0.972
	(5.31)	(4.46)		(27.6)	(5.41)		(332)	(97.0)	(49.9)	
5% GAC	2299	0.283	0.996	0.172	8120	0.898	56.01	48115	0.144	0.997
	(1.82)	(1.77)		(20.3)	(4.98)		(91.0)	(31.6)	(13.9)	
5% PAC	2131	0.279	0.995	0.203	7660	0.904	67.55	45952	0.141	0.995
	(2.35)	(2.15)		(21.7)	(4.68)		(149)	(50.7)	(23.5)	
10% GAC	4317	0.305	0.997	1.32	9108	0.921	165.9	65743	0.145	0.998
	(1.07)	(1.64)		(18.9)	(4.62)		(94.5)	(40.9)	(16.5)	
10% PAC	3726	0.312	0.989	0.611	9507	0.933	61.36	62882	0.153	0.995
	(1.99)	(2.56)		(15.2)	(4.49)		(104)	(47.6)	(19.6)	

AC = activated carbon; GAC = granular activated carbon; PAC = powdered activated carbon.
[a] Values in parentheses are standard errors (%); R^2 = coefficient of determination.

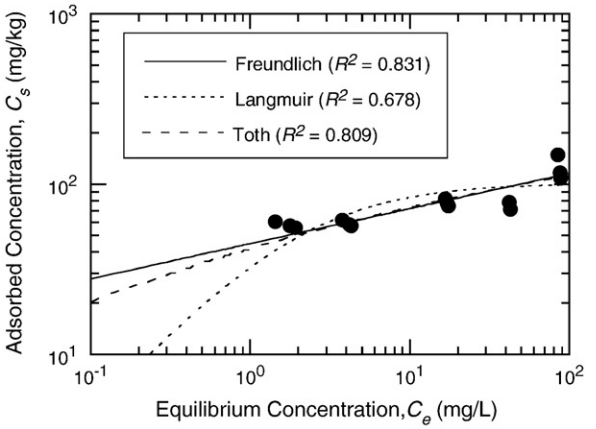

Fig. 2. Fitted adsorption models for phenol adsorption to unamended backfill mixture (see Table 3 for fitting parameters).

reached in the adsorption tests. Additional adsorption data corresponding to higher values of C_e than those shown in Fig. 3 would have been required in order to reduce the standard error associated with the fitted Q_T values. Thus, although the standard errors do not detract from the quality of the fits provided by the Tóth model over the range of equilibrium concentrations measured in the adsorption tests, the magnitudes of these errors caution against interpretation of the fitted Q_T values as true adsorption capacities.

Based on the aforementioned analyses, the Freundlich and Tóth models were considered equally plausible for representing phenol adsorption exhibited by the AC amended backfills within the range of the measured adsorption data. However, the results in Fig. 3 illustrate that the two models begin to deviate at $C_e \approx 1.0$ mg/L and deviate further when extrapolated to concentrations lower than those measured in the adsorption tests. This finding is consistent with a recent study by Matott et al. (2009) and is attributed to the differences in behavior of the adsorption model expressions as C_e approaches zero. The Tóth model approaches linear adsorption behavior as C_e approaches zero, with the limiting slope of the model being defined as follows based on Eq. (1):

$$\left.\frac{dC_s}{dC_e}\right|_{C_e \to 0} \approx K_d \tag{4}$$

where K_d ($=Q_T K_T$) is a linear distribution coefficient. In contrast, the Freundlich model predicts infinite affinity for the solute as C_e approaches zero (i.e., $dC_s/dC_e \to \infty$ as $C_e \to 0$), which is not valid from a thermodynamic standpoint (Tóth, 1995; Hinz, 2001). This difference in limiting slopes results in greater predicted adsorption by the Freundlich model relative to the Tóth model for aqueous concentrations below the range of measured adsorption data. As noted by Matott et al. (2009), differences in fitted model expressions at extrapolated concentrations may affect the outcome of transport simulations for adsorptive barriers in which the concentrations occurring within the barrier are outside the range of concentrations used for determining adsorption model parameters. Therefore, transport simulations were performed in this study using both the Freundlich and Tóth models so that the predictions of phenol transport could be compared.

3.2. Transport modeling

Transport of phenol through an SB vertical barrier was simulated using an advective-diffusive model that accounts for the nonlinear adsorption exhibited by the backfills. The governing mass-balance equation may be expressed in dimensionless form as follows for one-dimensional transport under local equilibrium conditions with steady flow:

$$r(u)\frac{\partial u}{\partial T^*} = \frac{\partial^2 u}{\partial X^2} - P_L \frac{\partial u}{\partial X} \tag{5}$$

where u is the normalized solute concentration (i.e., $u = C/C_o$, where C is the solute concentration within the pore fluid of the soil and C_o is the source concentration) and X is the normalized distance of transport through the barrier (i.e., $X = x/L$, where x is the distance of transport and L is the barrier thickness). The terms $r(u)$, T^*, and P_L in Eq. (5) are the retardation factor, dimensionless time, and dimensionless barrier Péclet number, respectively, defined as follows:

$$r(u) = 1 + \Lambda \frac{d\theta}{du}; \quad T^* = \frac{D_e t}{L^2}; \quad P_L = \frac{v_s L}{D_e} \tag{6}$$

where θ is the normalized solid-phase concentration ($\theta = C_s/C_{so}$, where C_s is the actual solid-phase concentration and C_{so} is the maximum solid-phase concentration), D_e is the effective diffusion coefficient ($D_e = \tau_a \cdot D_o$, where τ_a is the apparent tortuosity factor as defined by Shackelford and Daniel (1991) and D_o is the diffusion coefficient for the solute in aqueous solution), and t is time. The capacity ratio, Λ, and seepage velocity, v_s, are defined as follows:

$$\Lambda = \frac{\rho_d}{n} \cdot \frac{C_{so}}{C_o}; \quad v_s = \frac{ki}{n} \tag{7}$$

where ρ_d, n, and k are the dry density, porosity, and hydraulic conductivity of the SB backfill, respectively, and i is the hydraulic gradient across the barrier ($i = -\Delta h/L$, where Δh is the head difference across the barrier).

For the case of Freundlich adsorption, the maximum solid-phase concentration C_{so} is given by

$$C_{so} = K_F C_o^{N_F} \tag{8}$$

Thus, Λ and $r(u)$ can be expressed as follows:

$$\Lambda = \frac{\rho_d}{n} \cdot K_F C_o^{N_F - 1} \tag{9}$$

$$r(u) = 1 + \Lambda N_F u^{N_F - 1} = 1 + \frac{\rho_d}{n} K_F C_o^{N_F - 1} N_F u^{N_F - 1} \tag{10}$$

For the case of Tóth adsorption, C_{so} is given by

$$C_{so} = \frac{K_T Q_T C_o}{\left[1 + (K_T C_o)^{N_T}\right]^{1/N_T}} \tag{11}$$

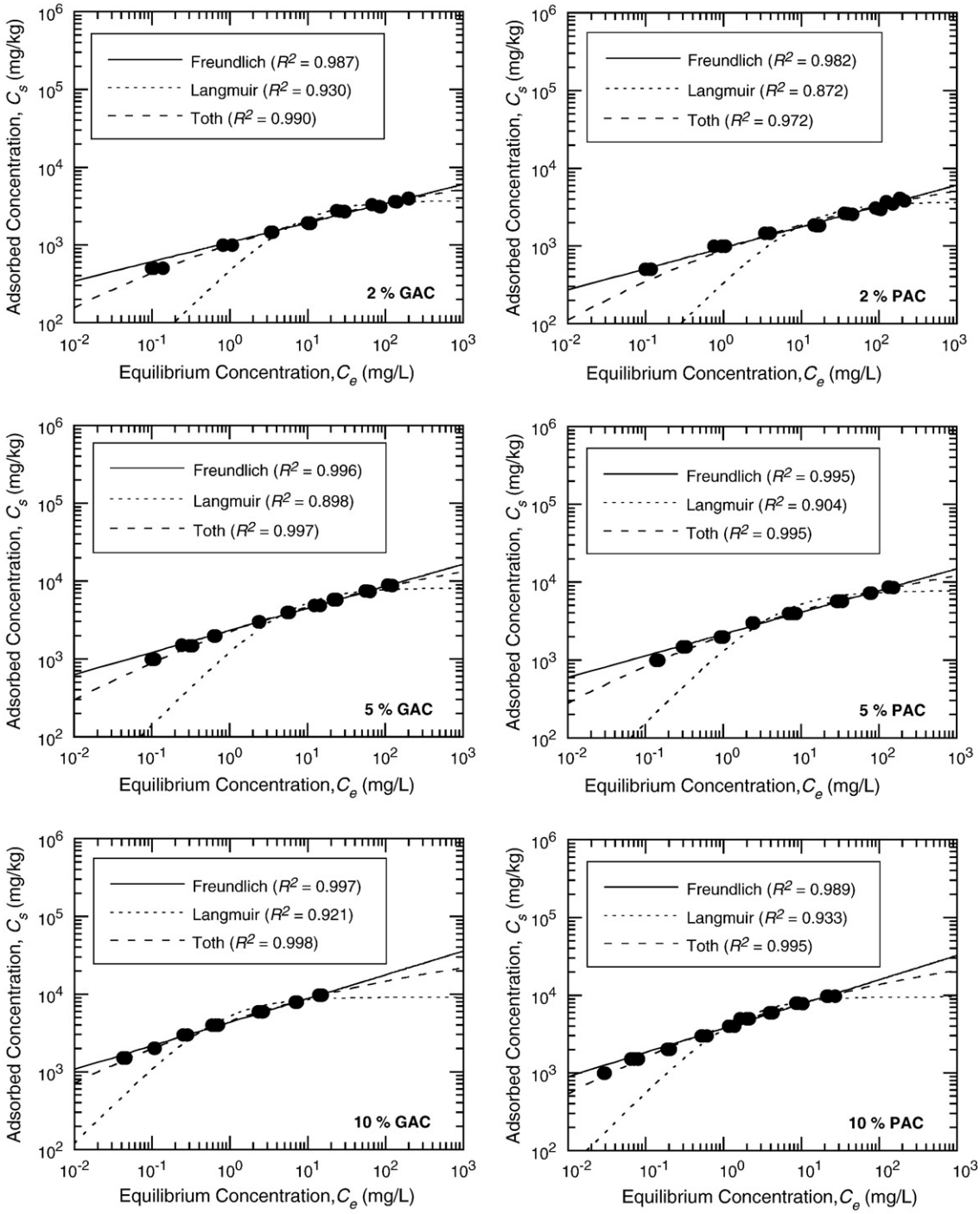

Fig. 3. Fitted adsorption models for phenol adsorption to backfill mixtures amended with either granular activated carbon (GAC) or powdered activated carbon (PAC) (see Table 3 for fitting parameters).

such that the resulting expressions for Λ and $r(u)$ are as follows:

$$\Lambda = \frac{\rho_d}{n} \cdot \frac{K_T Q_T}{\left[1 + (K_T C_o)^{N_T}\right]^{1/N_T}} \tag{12}$$

$$r(u) = 1 + \frac{\Lambda}{1 + (K_T C_o u)^{N_T}} \left[\frac{1 + (K_T C_o)^{N_T}}{1 + (K_T C_o u)^{N_T}}\right]^{1/N_T} = 1 + \frac{\rho_d}{n} K_T Q_T \left[1 + (K_T C_o u)^{N_T}\right]^{N_T/(1+N_T)} \tag{13}$$

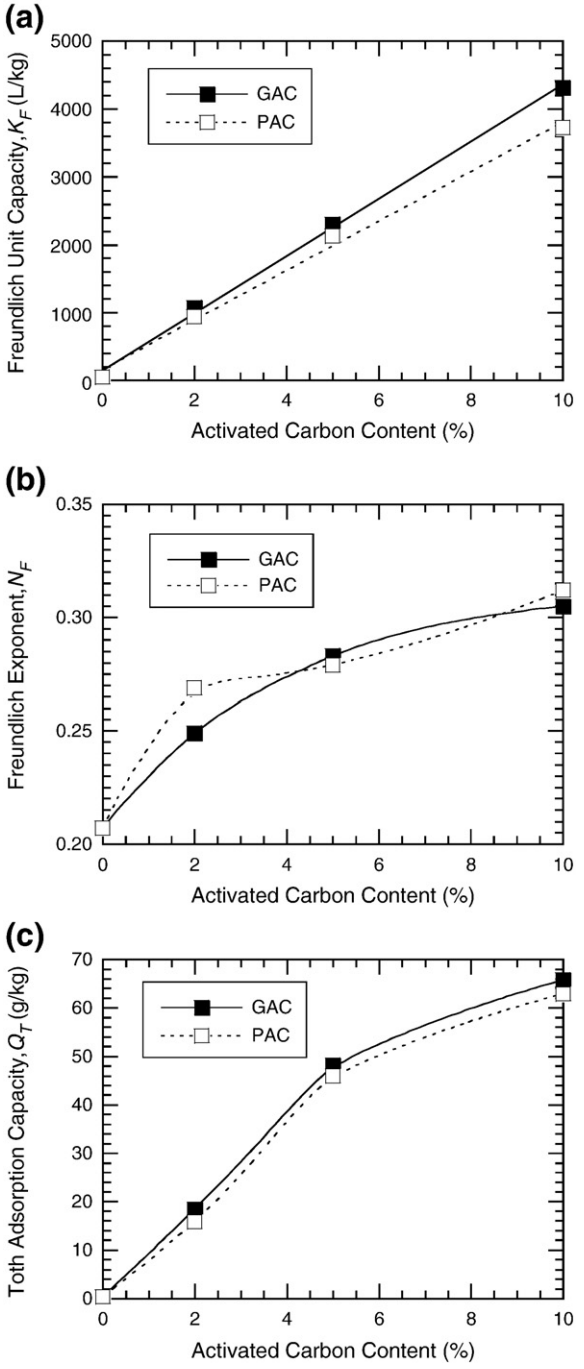

Fig. 4. Best-fit values of (a) Freundlich unit capacity, K_F, (b) Freundlich exponent, N_F, and (c) Tóth adsorption capacity, Q_T, for backfills amended with either granular activated carbon (GAC) or powdered activated carbon (PAC).

The governing equation for solute transport with Freundlich adsorption is obtained by substituting Eq. (10) into Eq. (5), whereas the governing equation for solute transport with Tóth adsorption is obtained by substituting Eq. (13) into Eq. (5).

The boundary conditions employed in the model simulations were a constant source entry boundary [$u(X=0,T^*)=1$] and a perfectly flushing exit boundary [$u(X=1,T^*)=0$]. Also, the initial concentration of phenol within the barrier was assumed to be zero [$u(X,T^*=0)=0$]. Similar boundary and initial conditions have been utilized in previous computational studies of pollutant transport through natural and engineered clay barriers (e.g., Greenberg et al., 1973; Rabideau and Khandelwal, 1998a; Malusis and Shackelford, 2002; Manassero and Dominijanni, 2003). In addition, the perfectly flushing exit boundary condition has been recommended as a conservative approach for design of vertical barriers (Rabideau and Khandelwal, 1998a).

The solutions herein are presented in terms of a dimensionless exit flux, $J^*(X=1,T^*)$, that is related to the exit mass flux of solute, $J(x=L,T^*)$, as follows:

$$J^*(X=1,T^*)=\frac{J(x=L,T^*)}{J_{ss}^d}=\frac{J(x=L,T^*)\cdot L}{nD_eC_o} \tag{14}$$

where J_{ss}^d ($=nD_eC_o/L$) is the steady-state diffusive mass flux. Thus, $J^*(X=1,T^*)$ represents a relative measure of the exit mass flux at a given time T^* compared to the theoretical mass flux that would occur through a barrier during steady-state transport under purely diffusive conditions. For example, the dimensionless flux at steady state, J_{ss}^*, is unity (i.e., $J_{ss}^*=1$) for the case of pure diffusion (i.e., $i=P_L=0$). For advective–diffusive transport (i.e., $i\neq 0$, $P_L\neq 0$), J_{ss}^* is related to P_L by the following expression:

$$J_{ss}^*=\frac{P_L}{1-exp(-P_L)} \tag{15}$$

Three different vertical barrier containment scenarios for a 1-m-thick SB barrier were considered in the model simulations, as illustrated in Fig. 5: (1) solute transport with advection occurring in the same direction as diffusion (i.e., co-advection; $i>0$, $P_L>0$); (2) purely diffusive solute transport ($i=P_L=0$); and (3) solute transport with advection occurring opposite to the direction of diffusion (i.e., counter-advection; $i<0$, $P_L<0$). The latter two scenarios, in particular, are relevant for vertical barrier systems in which the groundwater level on the source (contaminated) side of the barrier is lowered by pumping to eliminate the hydraulic gradient or to create an inward (reverse) gradient that reduces the outward diffusive flux. Based on Eq. (15), $J_{ss}^*>1$ for the co-advective case, whereas $0<J_{ss}^*<1$ for the counter-advective case.

The hydraulic gradient, i, used in the simulations ranged between $+1$ (co-advection) to -1 (counter-advection), corresponding to head differences, Δh, across the barrier of -1 and $+1$ m, respectively. The barrier hydraulic conductivity, k, was assumed to be 10^{-9} m/s in all cases, consistent with the typical design requirement that k be $\leq 10^{-9}$ m/s for vertical barriers used in geoenvironmental containment applications. Also, n and ρ_d were set at 0.5 and 1.325 Mg/m^3, respectively, based on testing performed by Malusis et al. (2009). Finally, $D_e=3.3\times10^{-10}$ m^2/s based on $D_o=9.4\times10^{-10}$ m^2/s for phenol (Castillo et al., 1992) and $\tau_a=0.35$, which is consistent with experimental results reported by Krol and Rowe (2004) for diffusion of TCE through SB backfill. Based on these input parameters and Eq. (6), values of P_L used in the simulations ranged from 6 (co-advection) to -6 (counter-

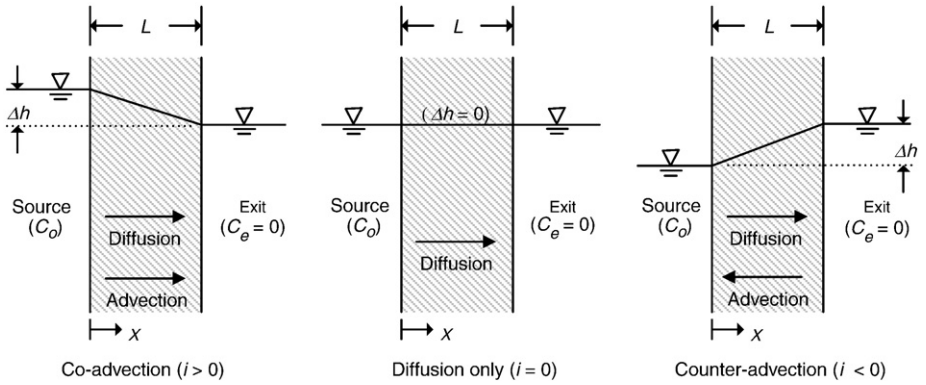

Fig. 5. Schematic illustration of vertical barrier containment scenarios considered in transport model simulations (adapted after Sleep et al., 2006).

advection). However, only $P_L = 6$ was used as the base scenario to examine the influence of AC type (GAC versus PAC) and adsorption model (Freundlich versus Tóth) on predicted phenol breakthrough.

The adsorption conditions considered in the model simulations are listed in Table 4 for the Freundlich model and the Tóth model, with values of capacity ratio, Λ, computed based on the fitting parameters in Table 3. The values of Λ in Table 4 correspond to one of the three different values of source concentration, C_o (= 0.1, 1 and 10 mg/L), that were considered in the model simulations. The Λ values for a given adsorption model (Freundlich or Tóth) and AC content decrease with increasing C_o, reflecting the concavity of the adsorption data. Also, values of Λ corresponding to a given C_o increased with increasing AC content and were slightly higher for the GAC-amended backfills relative to backfills amended with the same percentage of PAC.

For the case of transport through an unamended barrier (0% AC), an additional transport simulation was considered in which the barrier was nonreactive (i.e., $\Lambda = 0$). The nonreactive simulation represented a limiting condition for unamended SB backfill in which solute retention was nil. As discussed previously, appreciable phenol retention by the control backfill tested in this study may be attributed to interactions with the bentonite component of the backfill that comprised 5.8 wt.% of the dry solids mass. Such interactions with bentonite do not appear to be significant for all VOCs based on the aforementioned adsorption studies by Gullick (1998), Khandelwal et al. (1998), and Krol and Rowe (2004). Also, the bentonite content in SB backfill may be as low as 1% (i.e., the contribution of bentonite from the slurry) if the native soil contains adequate fines to achieve the required hydraulic conductivity without dry bentonite amendment (Sharma and Reddy, 2004). In such cases, phenol retention by unamended backfill may be considerably lower than observed in this study.

Model simulations were performed by solving Eq. (5) numerically using the *MATLAB* (Mathworks, Inc., Natick, MA) partial differential equation (PDE) solver (pdepe). This numerical PDE solver converts PDEs to ordinary differential equations (ODEs) using a piecewise nonlinear Galerkin/Petrov–Galerkin method (Skeel and Berzins, 1990) that is second-order accurate in space. The time integration then was performed by an ODE solver (ode15s) that changes the time step dynamically. The absolute and relative error tolerances of the solver were set to 10^{-8}, and the barrier was discretized using 300 nodes spaced logarithmically such that the nodes were closely spaced near the entry and exit boundaries of the barrier. To avoid the computational difficulties with the infinite limiting slope of the Freundlich model, a non-zero initial concentration (u_i) of 10^{-8} was assigned at all nodes within the barrier. Computational accuracy of the *MATLAB* model was ensured by comparing the model against analytical solutions based on linear

Table 4
Values of capacity ratio, Λ, for Freundlich and Tóth adsorption conditions as a function of source concentration (C_o = 0.1, 1, 10 mg/L).

Adsorption model	C_o	Capacity ratio, Λ[a]						
	(mg/L)	0% AC	2% GAC	2% PAC	5% GAC	5% PAC	10% GAC	10% PAC
Freundlich	0.1	732	16,000	13,400	31,800	29,700	56,700	48,100
	1	118	2840	2480	6090	5650	11,400	9870
	10	19.0	504	461	1170	1070	2310	2030
Tóth	0.1	542	11,300	9110	23,300	21,627	51,800	41,300
	1	111	2640	2320	5820	5360	11,900	10,100
	10	19.5	523	488	1220	1120	2300	2060

AC = activated carbon; GAC = granular activated carbon; PAC = powdered activated carbon.
[a] Computed using $n = 0.5$, $\rho_d = 1.325$ Mg/m^3, and the best-fit adsorption parameters in Table 3.

adsorption (i.e., Crank, 1975; Rabideau and Khandelwal, 1998a) over the range $-10 \leq P_L \leq 10$.

3.2.1. Flux breakthrough curves

The dimensionless flux breakthrough curves for $P_L = 6$ are shown in Fig. 6 as a function of source concentration, C_o, based on Freundlich and Tóth adsorption models. The flux breakthrough curve for the nonreactive case ($\Lambda = 0$) also is shown in Fig. 6 for comparison. The results indicate that a significant delay in first arrival of the phenol flux at the exit boundary (i.e., three to five orders of magnitude in terms of T^*) may occur for an AC amended SB cutoff wall relative to the nonreactive case in which phenol retention by the bentonite fraction is nil. The delay in first arrival increases with increasing AC content and decreases with increasing C_o, as expected based on the Λ values in Table 4. Also, a delay of approximately one to three orders of magnitude may be realized for the base case of unamended but reactive backfill (i.e., the 0% GAC/PAC curves in Fig. 6) relative to the nonreactive case, based on the intrinsic phenol retention exhibited by the control backfill (see Fig. 2). This apparent benefit may not be as significant for other VOCs or for SB barriers with a lower bentonite content, as discussed previously.

The results in Fig. 6 further show that both the Freundlich and Tóth breakthrough curves exhibit steeper fronts relative to the nonreactive case. The steeper fronts are a well-recognized effect of concave, nonlinear adsorption on solute transport, whereby the effect of nonlinear adsorption is to counteract solute dispersion due to diffusion (e.g., van Genuchten and Cleary, 1982; Shackelford, 1993). The Freundlich and Tóth breakthrough curves for a given AC content are similar at the higher source concentrations ($C_o = 1$ mg/L and 10 mg/L). However, at the lowest source concentration ($C_o = 0.1$ mg/L), the Tóth model yields a wider (more dispersed) front than the Freundlich model. As a result, the Tóth model yields lower flux breakthrough times relative to the Freundlich model for $C_o = 0.1$ mg/L.

The wider fronts exhibited by the Tóth breakthrough curves relative to the Freundlich breakthrough curves for $C_o = 0.1$ mg/L in Fig. 6 are attributed to lower slopes of the fitted Tóth model expressions relative to the fitted Freundlich model expressions for $C_e < 0.1$ mg/L (see Fig. 3). Since the

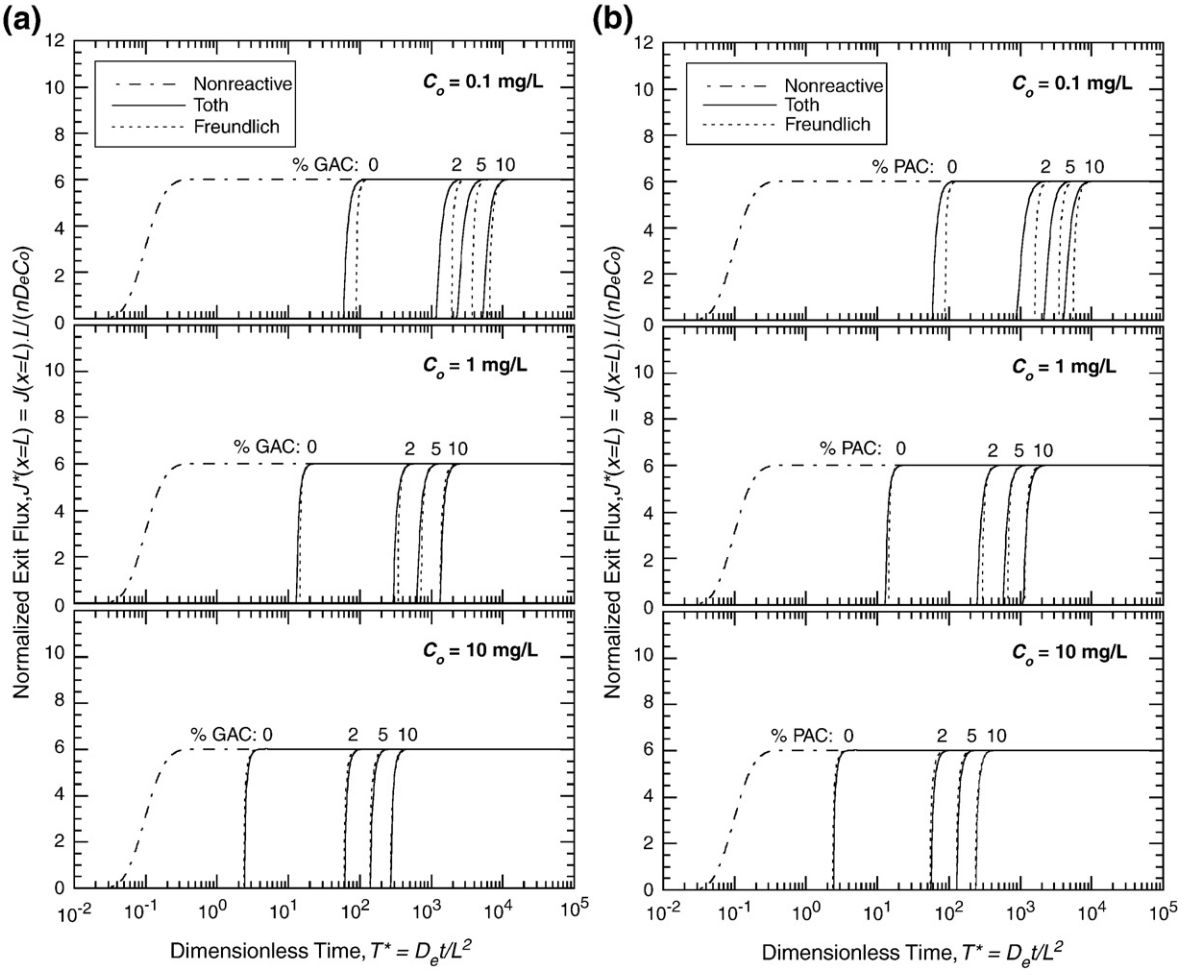

Fig. 6. Comparison of predicted flux breakthrough curves for SB cutoff wall ($P_L = 6$) based on different adsorption models (nonreactive, Tóth, Freundlich) as a function of the content of (a) granular activated carbon (GAC) or (b) powdered activated carbon (PAC).

finite limiting slope of the Tóth model is more thermodynamically consistent than the infinite limiting slope of the Freundlich model, the Tóth breakthrough curves are considered more realistic than the Freundlich breakthrough curves for $C_o = 0.1$ mg/L. However, the slopes of the two models are similar for phenol concentrations greater than 0.1 mg/L that are within the range of measured C_e in the adsorption tests. As a result, only a slight difference between the Tóth and Freundlich breakthrough curves is evident in Fig. 6 for $C_o = 1$ mg/L, and virtually no difference is evident for $C_o = 10$ mg/L.

3.2.2. Flux breakthrough time

Predicted values of the dimensionless flux breakthrough time, T_B^*, are plotted in Fig. 7 as a function of GAC or PAC content. In Fig. 7, T_B^* is defined as the dimensionless time corresponding to an exit flux, J^*, equal to 5% of the steady-state exit flux, J_{ss}^*, or

$$T_B^* = T^*\left[\left(J^*/J_{ss}^*\right)_{x=L} = 0.05\right] \tag{16}$$

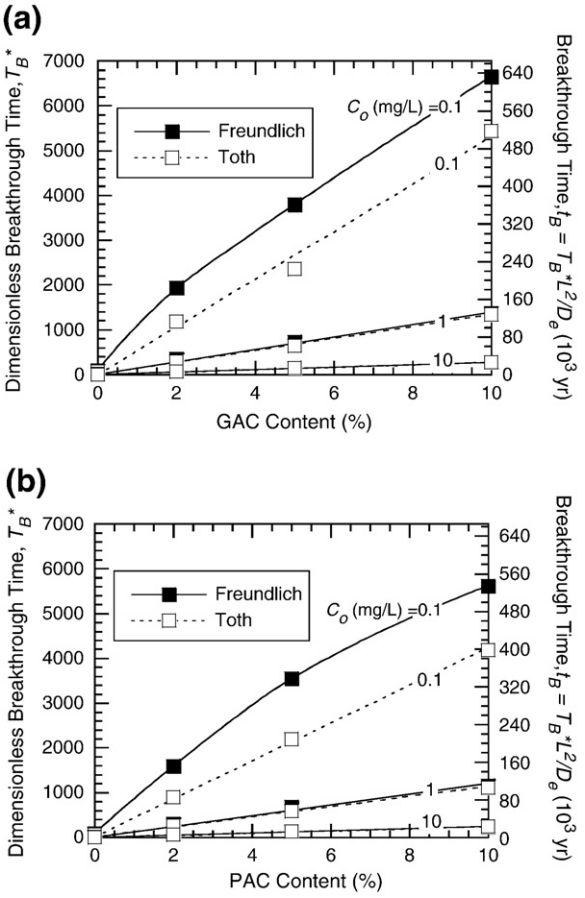

Fig. 7. Predicted flux breakthrough times ($P_L = 6$) for backfills containing (a) granular activated carbon (GAC) and (b) powdered activated carbon (PAC). Symbols represent predicted breakthrough times for GAC or PAC contents of 0, 2, 5, and 10% based on the breakthrough curves in Fig. 6.

This definition of T_B^* was chosen as a practical representation of first arrival of the phenol flux at the exit boundary. Although T_B^* could be defined based on a different percentage of the steady-state flux (e.g., 50%), the resulting values of T_B^* would not be markedly different given the steep fronts associated with the Freundlich and Tóth breakthrough curves in Fig. 6. The dimensional breakthrough times, t_B, corresponding to these values of T_B^* (computed using Eq. (6)) also are shown in Fig. 7 and are listed in Table 5.

The results in Table 5 show that t_B is approximately 4.3 yr for a nonreactive SB barrier based on $L = 1$ m, $P_L = 6$, and T_B^* as defined by Eq. (16). In contrast, t_B for the unamended SB barrier (0% AC) ranges from ~230 yr ($C_o = 10$ mg/L) to more than 8500 yr ($C_o = 0.1$ mg/L), while t_B for a SB barrier containing up to 10% GAC or PAC may range from ~5800 yr ($C_o = 10$ mg/L) to more than 600,000 yr ($C_o = 0.1$ mg/L). The magnitudes of the predicted t_B values for the AC amended barriers illustrate that AC amendment may offer a significant benefit in terms of enhanced VOC containment by SB barriers, provided that the local equilibrium conditions and resulting measured adsorption properties obtained in the adsorption tests are representative of the conditions and properties that would exist in the field. If so, the results in this study suggest that, for phenol, AC amendments less than 2% (or even no AC amendment, depending on the bentonite content in the backfill) may provide sufficient adsorption to prevent phenol breakthrough for hundreds or even thousands of years.

The results in Fig. 7 reinforce the aforementioned observations from the breakthrough curves in Fig. 6 that breakthrough time increases with increasing AC content and decreasing C_o, with the Tóth model yielding similar or earlier breakthrough relative the Freundlich model for a given AC content and C_o. The increase in predicted breakthrough time with increasing AC content is reasonably linear over the range of AC contents considered in the study. Also, t_B is insensitive to C_o for a nonreactive barrier, but decreases log-linearly with increasing C_o for an unamended or AC-amended SB barrier as illustrated in Fig. 8. The decrease in t_B with increasing C_o is due to a reduction in the nonlinear retardation factor with increasing pore-water concentration (see Eqs. (10) and (13)). Finally, the results in Fig. 7 show that, for a given AC content, little difference in T_B^* (or t_B) is predicted for GAC amended backfill relative to PAC amended backfill.

The insensitivity of T_B^* to AC type is consistent with the similar adsorption parameters (Table 3) and Λ values (Table 4) for GAC amended backfills and PAC amended backfills for the same AC content. From a practical standpoint, this finding indicates that selection of GAC or PAC as a SB barrier amendment may be driven by factors other than adsorption, such as the cost of the amendment and the influence of the amendment on barrier hydraulic conductivity. The bulk unit costs provided by the vendors for the PAC and GAC used in this study were \$1.65/kg and \$7.50/kg, respectively. Thus, for a 10-m-deep, 1-m-thick SB cutoff wall, the cost for AC amendment of 2 wt% (assuming a porosity of 0.5 and a specific gravity of solids of 2.65) would amount to approximately \$400 for PAC and \$2000 for GAC per meter length of wall. In addition, Malusis et al. (2009) showed that addition of PAC caused a decrease in hydraulic conductivity of the backfill relative to the unamended backfill mixture, whereas addition of GAC had no effect on hydraulic

Table 5
Summary of predicted flux breakthrough times for 1-m-thick SB barrier ($P_L = 6$) as a function of adsorption model (nonreactive, Freundlich, and Tóth) and source concentration ($C_o = 0.1$, 1, 10 mg/L).

Adsorption model	C_o (mg/L)	Flux breakthrough time, t_B (yr)						
		0% AC	2% GAC	2% PAC	5% GAC	5% PAC	10% GAC	10% PAC
Nonreactive	0.1	4.29	–	–	–	–	–	–
	1	4.29	–	–	–	–	–	–
	10	4.29	–	–	–	–	–	–
Freundlich	0.1	8520	184,000	151,000	361,000	338,000	632,000	534,000
	1	1380	32,900	28,400	69,100	64,400	130,000	128,000
	10	229	5820	5290	13,200	12,300	25,900	22,500
Tóth	0.1	5690	112,000	86,000	224,000	209,000	517,000	398,000
	1	1250	28,300	24,000	60,500	56,000	128,000	106,000
	10	235	5890	5430	13,500	12,400	26,100	22,500

AC = activated carbon; GAC = granular activated carbon; PAC = powdered activated carbon.

conductivity. Based on these additional considerations, PAC appears to offer better value than GAC as a barrier amendment.

3.2.3. Influence of Péclet number on flux breakthrough

Dimensionless flux breakthrough curves for a 1-m-thick SB barrier ($C_o = 1$ mg/L) with P_L ranging from 6 to −6 are shown in Fig. 9 for a nonreactive barrier, an unamended (i.e., 0% AC) but reactive barrier (Tóth model), and a reactive barrier amended with 2% PAC (Tóth model). The results in Fig. 9 show that a decrease in P_L causes an increasing delay in first arrival of the phenol flux due to the reduction and/or reversal of the advective component of the flux. However, the primary advantage of pumping to lower or reverse the hydraulic gradient is a reduction in the steady-state exit flux. For example, $J^*_{ss} \approx 6$ for the case of co-advection with $P_L = 6$, but reduced to $J^*_{ss} \approx 0.015$ for the case of counter-advection with $P_L = -6$ (see Eq. (15)).

Since different values of P_L result in different values of J^*_{ss}, the influence of P_L on flux breakthrough time is examined by defining t_B as the time corresponding to a prescribed value of J^* rather than a prescribed percentage of J^*_{ss}. In this case, t_B is defined as the time corresponding to $J^* = 0.015$, or 100% of the steady-state flux for $P_L = -6$ (see Fig. 9). The resulting values of t_B are plotted as a function of P_L and hydraulic gradient, i, in Fig. 10. Comparison of t_B values in Fig. 10 for a nonreactive SB barrier with those for an SB barrier containing 2% PAC indicates that the delay in breakthrough associated with lowering P_L is negligible relative to the delay in breakthrough caused by hydrophobic partitioning to the PAC. However, the results in Fig. 10 also show that similar values of t_B are predicted for an unamended SB barrier (0% PAC) with $P_L = -6$ and a 2% PAC amended SB barrier with $P_L = 6$. These findings illustrate that, from the standpoint of breakthrough time, the benefit of amending an SB barrier with AC relative to the benefit associated with pumping to reverse the hydraulic gradient will largely depend upon the attenuation capacity of the non-AC fraction of the barrier and the magnitude of the Péclet number associated with the reverse gradient.

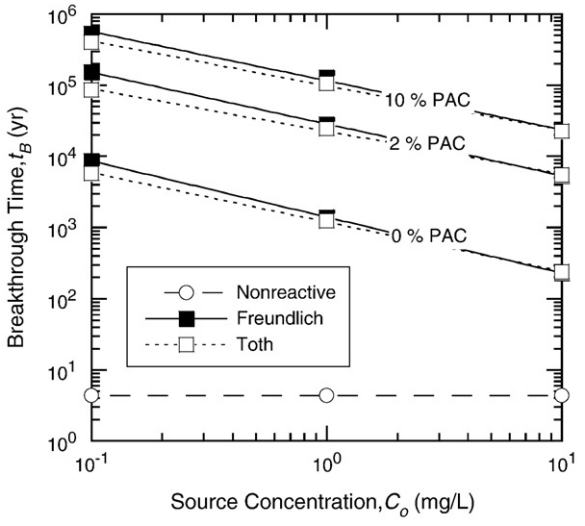

Fig. 8. Influence of source concentration, C_o, on predicted flux breakthrough time ($P_L = 6$) for barriers amended with powdered activated carbon (PAC).

The transport of phenol through an SB barrier based on the model simulations conducted in this study can be considered representative of the expected transport in the field only if the adsorption behavior based on the results of the adsorption tests is representative. In particular, the simulated predictions of phenol breakthrough time inherently are based on the assumption that local equilibrium is established between the liquid and solid phases during solute transport. Such predictions would be unconservatively high (slow) for systems in which adsorption occurs under nonequilibrium (kinetically limited) conditions (Brusseau and Rao, 1989a,b; Weber et al., 1991; Rabideau and Khandelwal, 1998b). Rabideau and Khandelwal (1998b) indicate that, although nonequilibrium conditions are unlikely to influence the performance of a 1-m-thick SB cutoff wall under typical field conditions, model simulations based on equilibrium adsorption should be viewed with caution due to potential for unconservative prediction of barrier performance in cases where the local equilibrium assumption is inappropriate. In addition, the dependency of measured adsorption on the solid:solution ratio (SSR) employed in the adsorption tests has been well established (e.g., Limousin et al., 2007). An SSR of 1:10 was deemed to be the lowest feasible SSR for the tests conducted in this study. In contrast, the SSR for saturated SB

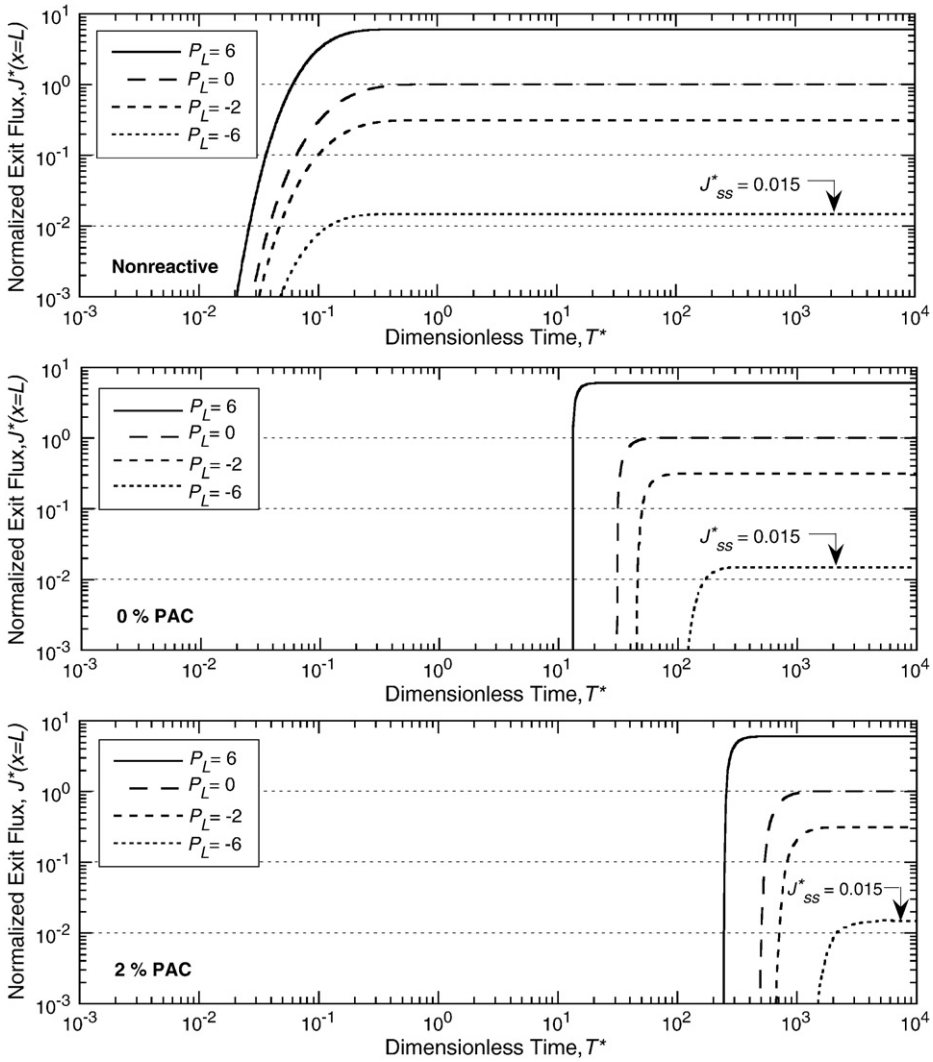

Fig. 9. Effect of Péclet number, P_L, on flux breakthrough curves ($C_o = 1$ mg/L) for a nonreactive barrier, an unamended but reactive barrier (Tóth model), and a reactive barrier amended with 2% powdered activated carbon (PAC) (Tóth model).

backfill in a constructed cutoff wall is expected to be on the order of 1:0.4 (assuming a porosity of 0.5 and a specific gravity of solids of 2.65). Based on these considerations, column testing performed using field hydrodynamic conditions and more representative SSRs is warranted to verify or refine the results of an equilibrium testing approach.

4. Conclusions

The results of equilibrium adsorption tests and solute transport model simulations performed to determine the potential for enhanced phenol adsorption in an activated carbon (AC) amended soil–bentonite (SB) vertical barrier were presented. The adsorption test results for model SB backfills amended with 0 to 10 wt.% granular AC (GAC) or powdered AC (PAC) indicated that all of the backfills, including the unamended backfill (0% AC), exhibited nonlinear phenol adsorption best described by the Freundlich or Tóth adsorption model. The adsorption capacity of the AC amended backfills was substantially greater than the adsorption capacity of the unamended backfill and increased with increasing AC content. The GAC and PAC provided similar adsorption enhancement, despite the relative differences in particle size, presumably due to the similar total (internal plus external) specific surfaces measured for the GAC and PAC. The unamended backfill also exhibited modest phenol retention attributed to interactions between phenol and the bentonite component of the backfill (5.8 wt.%).

Based on the solute transport modeling results, an AC amendment ranging from 2 to 10 wt.% has the potential to increase phenol breakthrough time through a 1-m-thick SB barrier by several orders of magnitude when compared to the case of a nonreactive barrier. Breakthrough time increased linearly with increasing AC content but decreased log-linearly with increasing source concentration due to a reduction in the nonlinear retardation factor with increasing pore-water concentration. The delay in breakthrough realized by AC amendment will likely be greater than a delay in breakthrough

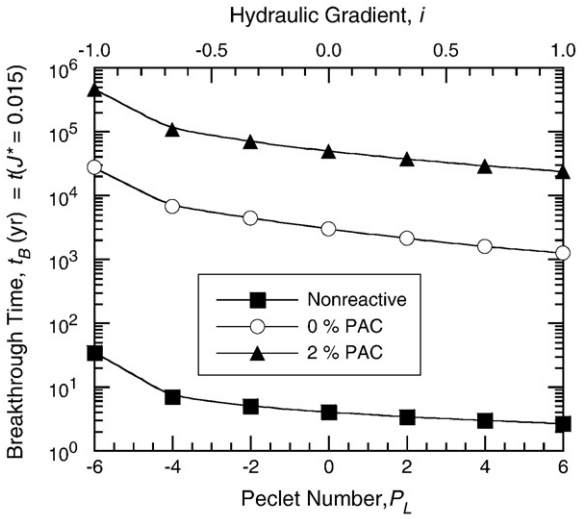

Fig. 10. Relationship between Péclet number, P_L, and predicted flux breakthrough times ($C_o = 1$ mg/L) for a nonreactive barrier, an unamended but reactive barrier (Tóth model), and a reactive barrier amended with 2% powdered activated carbon (PAC) (Tóth model). Note: plotted breakthrough times correspond to $J^*(x = L) = 0.015$.

realized by pumping to lower or reverse the hydraulic gradient across the barrier, depending upon the AC content, the magnitude and direction of the hydraulic gradient, and the intrinsic adsorption capacity of the non-AC solids in the backfill. In this study, an increase in phenol breakthrough time of one to three orders of magnitude was predicted for an unamended barrier due to the intrinsic phenol retention capacity observed in the adsorption test for the unamended backfill. This benefit may be less significant for other VOCs or for SB barriers with lower bentonite contents. Nonetheless, the results illustrate that the intrinsic VOC adsorption capacity of the native soil and bentonite in the backfill may be appreciable for certain VOCs and should be considered when determining the need for an adsorptive amendment.

The modeling results also indicated that the Freundlich and Tóth models generally yielded similar predicted breakthrough times. However, the Tóth model may be more conservative (i.e., yield lower breakthrough times relative to the Freundlich model) at low source concentrations due to greater spreading of the solute front. The greater spreading was attributed to the lower slope of the Tóth isotherm relative to the Freundlich isotherm at solute concentrations approaching zero.

Overall, the results of this study indicate that AC may be a highly effective amendment for enhancing phenol adsorption capacity of an SB barrier. Similar or greater adsorption also may be realized for other VOCs with similar or greater affinity for hydrophobic partitioning to the AC phase. The coupling of equilibrium adsorption tests with a local equilibrium transport model is useful as a simple platform for screening the containment performance of AC amended and unamended SB barriers for a particular VOC or combination of VOCs. However, column testing based on representative hydrodynamic conditions and solid:solution ratios should be considered as part of a final design process for an AC amended SB barrier to verify or refine the results of an equilibrium testing approach.

Acknowledgments

Financial support for this study was provided by the U. S. National Science Foundation (NSF), Arlington, VA, under Grant CMS-0625159. The opinions expressed in this paper are solely those of the writers and are not necessarily consistent with the policies or opinions of the NSF. The authors thank Central Builders Supply (Lewisburg, PA) and Wyo-Ben (Billings, MT) for donating materials used in this study.

References

Allen, S.J., McKay, G., Porter, J.F., 2004. Adsorption isotherm models for basic dye adsorption by peat in single and binary component systems. J. Colloid Interface Sci. 280 (2), 322–333.

Banat, F.A., Al-Bashir, B., Al-Asheh, S., Hayajneh, O., 2000. Adsorption of phenol by bentonite. Environ. Pollut. 107 (3), 391–398.

Barben, E.J., Malusis, M.A., Evans, J.C., 2008. Slump evaluation of soil–bentonite backfill amended with activated carbon. Proc. GeoCongress 2008, Geotechnics of Waste Management and Remediation, ASCE GSP 177 ASCE, Reston, VA, pp. 636–643.

Bartelt-Hunt, S.L., Smith, J.A., Burns, S.E., Rabideau, A.J., 2005. Evaluation of granular activated carbon, shale and two organoclays for use as sorptive amendments in clay landfill liners. J. Geotech. Geoenviron. Engrg. 131 (7), 848–859.

Bierck, B.R., Chang, W.C., 1994. Contaminant transport through soil–bentonite slurry walls: attenuation by activated carbon. Proc., Water Environ. Fed. Specialty Conf. Water Environment Federation, Alexandria, VA, pp. 461–472.

Brusseau, M.L., Rao, P.S., 1989a. Sorption nonideality during organic contaminant transport in porous media. CRC Crit. Rev. Environ. Control 19 (1), 33–99.

Brusseau, M.L., Rao, P.S., 1989b. The influence of sorbate–organic matter interactions on sorption nonequilibrium. Chemosphere 18 (9/10), 1690–1706.

Castillo, R., Garza, C., Orozco, J., 1992. Mutual diffusion coefficients in the water-rich region of water/phenol mixtures and their relation to aggregate formation. J. Phys. Chem. 96 (3), 1475–1478.

Chern, J.-M., Chien, Y.-W., 2002. Adsorption of nitrophenol onto activated carbon: isotherms and breakthrough curves. Water Res. 36 (3), 647–655.

Chiang, Y.-C., Chiang, P.-C., Chang, E.-E., 2001. Effects of surface characteristics of activated carbons on VOC adsorption. J. Environ. Engrg., 127 (1), 54–62.

Chuang, C.-L., Chiang, P.-C., Chang, E.-E., 2003. Kinetics of benzene adsorption onto activated carbon. Environ. Sci. Pollut. Res. 10 (1), 6–8.

Crank, J., 1975. The Mathematics of Diffusion, 2nd ed. Clarendon Press, Oxford. 414 pp.

D'Appolonia, D.J., 1980. Soil–bentonite slurry trench cutoffs. J. Geotech. Engrg., 106 (4), 399–417.

Evans, J.C., 1994. Hydraulic conductivity of vertical cutoff walls. In: Daniel, D.E., Trautwein, S.J. (Eds.), Hydraulic Conductivity and Waste Contaminant Transport in Soils, ASTM STP 1142. ASTM, West Conshohocken, PA, pp. 79–94.

Greenberg, J.A., Mitchell, J.K., Witherspoon, P.A., 1973. Coupled salt and water flows in a groundwater basin. J. Geophys. Res. 78 (27), 6341–6353.

Gullick, R.W., 1998. Effects of sorbent addition on the transport of inorganic and organic chemicals in soil–bentonite cutoff wall containment barriers. *PhD Dissertation*, Department of Civil Engineering, University of Michigan, Ann Arbor, MI.

Gullick, R.W., Weber, W.J., 2001. Evaluation of shale and organoclays as sorbent additives for low-permeability soil containment barriers. Environ. Sci. Technol. 35 (7), 1523–1530.

Gullick, R.W., Weber, W.J., Gray, D.H., 1996. Organic transport through clay liners and slurry walls. In: Sahwney, B. (Ed.), CMS Workshop Lectures. Organic Pollutants in the Environment, Vol. 8. Clay Minerals Society, Boulder, CO, pp. 95–136.

Harmsen, K., 1982. Theories of cation adsorption by soil constituents: discrete-site models. In: Bolt, G.H. (Ed.), Soil Chemistry B. Physico-Chemical Models. Elsevier, New York, NY, pp. 77–140. Ch. 4.

Heilshorn, E.D., 1991. Removing VOCs from contaminated water. Chem. Engrg. 98 (2), 120–124.

Hinz, C., 2001. Description of sorption data with isotherm equations. Geoderma 99 (3-4), 225–243.
Ho, Y.S., Porter, J.F., McKay, G., 2002. Equilibrium isotherm studies for the sorption of divalent metal ions onto peat: copper, nickel and lead single component systems. Water, Air, Soil Pollut. 141 (1–4), 1–33.
Khandelwal, A., Rabideau, A.J., 2000. Enhancement of soil–bentonite barrier performance with the addition of natural humus. J. Contam. Hydrol. 45 (3–4), 267–282.
Khandelwal, A., Rabideau, A.J., Shen, P., 1998. Analysis of diffusion and sorption of organic solutes in soil–bentonite barrier materials. Environ. Sci. Technol. 32 (9), 1333–1339.
Kinniburgh, D.G., 1986. General purpose adsorption isotherms. Environ. Sci. Technol. 20 (9), 895–904.
Kong, E.J., DiGiano, F.A., 1986. Competitive adsorption among VOCs on activated carbon and carbonaceous resin. J. Am. Water Works Assoc. 78 (4), 181–188.
Krol, M.M., Rowe, R.K., 2004. Diffusion of TCE through soil–bentonite slurry walls. Soil Sed. Contam. 13 (1), 81–101.
LaGrega, M.L., Buckingham, P.L., Evans, J.C., 2001. Hazardous Waste Management, 2nd Ed. McGraw-Hill, New York, NY. 1202 pp.
Lake, C.B., Rowe, R.K., 2005. A comparative assessment of volatile organic compound (VOC) sorption to various types of potential GCL bentonites. Geotex. Geomem. 23 (4), 323–347.
Limousin, G., Gaudet, J.-P., Charlet, L., Szenknect, S., Barthes, V., Krimissa, M., 2007. Sorption isotherms: a review on physical bases, modeling and measurement. Appl. Geochem. 22 (2), 249–275.
Lo, I.M.-C., 2001. Organoclay with soil–bentonite admixture as waste containment barriers. J. Environ. Engrg. 127 (8), 756–759.
Malusis, M.A., Scalia, J., 2007. Hydraulic conductivity of an activated carbon-amended geosynthetic clay liner. Proc., Geo-Denver 2007, New Peaks in Geotechnics, ASCE GSP 163, ASCE, Reston, VA (CD-ROM).
Malusis, M.A., Shackelford, C.D., 2002. Theory for reactive solute transport through clay membrane barriers. J. Contam. Hydrol. 59 (3–4), 291–316.
Malusis, M.A., Barben, E.J., Evans, J.C., 2009. Hydraulic conductivity and compressibility of a model soil–bentonite backfill amended with activated carbon. J. Geotech. Geoenviron. Engrg., 131 (5), 664–672.
Manassero, M., Dominijanni, A., 2003. Modeling the osmosis effect on solute migration through porous media. Geotechnique 53 (5), 481–492.
Matott, L.S., Bandilla, K., Rabideau, A.J., 2009. Incorporating nonlinear isotherms into robust multilayer sorptive barrier design. Adv. Water Resour. 32 (11), 1641–1651.
Millet, R.A., Perez, J.-Y., Davidson, R.R., 1992. USA practice slurry wall specifications 10 years later. In: Paul, D.B., Davidson, R.R., Cavalli, N.J. (Eds.), Slurry Walls: Design, Construction and Quality Control, ASTM STP 1129. ASTM, West Conshohocken, PA, pp. 42–66.
Mott, H.V., Weber, W.J., 1992. Sorption of low molecular weight organic contaminants by fly ash: considerations for the enhancement of cutoff barrier performance. Environ. Sci. Technol. 26 (6), 1234–1242.
Neville, C.J., Andrews, C.B., 2006. Containment criterion for contaminant isolation by cutoff walls. Ground Water 44 (5), 682–686.
Park, J.K., Kim, J.Y., Madsen, C.D., Edil, T.B., 1997. Retardation of volatile organic compound movement by a soil–bentonite slurry cutoff wall amended with ground tires. Water Environ. Res. 69 (5), 1022–1031.
Peel, R.G., Benedek, A., 1980. Attainment of equilibrium in activated carbon isotherm studies. Environ. Sci. Technol. 14 (1), 66–71.
Prince, M.J., Maneval, J.E., Evans, J.C., 2000. Analysis of boundary conditions for contaminant transport through adsorptive, low-permeability slurry trench cutoff walls. In: Zimmie, T.F. (Ed.), GeoDenver 2000, ASCE GSP 105. ASCE, Reston, VA, pp. 58–72.
Rabideau, A.J., Khandelwal, A., 1998a. Boundary conditions for modeling transport in vertical barriers. J. Environ. Engrg., 124 (11), 1135–1139.
Rabideau, A.J., Khandelwal, A., 1998b. Nonequilibrium sorption in soil/bentonite barriers. J. Environ. Engrg., 124 (4), 329–335.
Rowe, R.K., Booker, J.R., Fraser, M.J., 1994. POLLUTE Version 6.0 User's Guide. GAEA Environ. Engrg., Ltd, London.
Rowe, R.K., Quigley, R.M., Booker, J.R., 1995. Clayey Barrier Systems for Waste Disposal Facilities. E & FN SPON, London. 390 pp.
Roy, W.R., Krapac, I.G., Chou, S.F.J., Griffin, R.A., 1992. Batch-type Procedures for Estimating Soil Adsorption of Chemicals. U. S. Environmental Protection Agency, Washington, D.C. EPA/530/SW-87/006-F, 100 pp.
Rumer, R.R., Ryan, M.R., 1995. Barrier Containment Technologies for Environmental Remediation Applications. Wiley, New York, NY. 170 pp.
Ryan, C.R., 1987. Vertical barriers in soil for pollution containment. In: Woods, R. (Ed.), Geotechnical Practice for Waste Disposal '87, ASCE GSP 13 ASCE, Reston, VA, pp. 182–204.
Shackelford, C.D., 1993. Chapter 3: contaminant transport. In: Daniel, D.E. (Ed.), Geotechnical Practice for Waste Disposal. Chapman and Hall, London, pp. 33–65.
Shackelford, C.D., Daniel, D.E., 1991. Diffusion in saturated soil. 1. Background. J. Geotech. Engrg., 117 (3), 467–484.
Shackelford, C.D., Redmond, P., 1995. Solute breakthrough curves for processed kaolin at low flow rates. J. Geotech. Engrg. 121 (1), 17–32.
Sharma, H.D., Reddy, K.R., 2004. Geoenvironmental Engineering. Wiley, Hoboken, NJ. 968 pp.
Skeel, R.D., Berzins, M., 1990. A method for the spatial discretization of parabolic equations in one space variable. SIAM J. Sci. Stat. Comput. 11 (1), 1–32.
Sleep, B.E., Shackelford, C.D., and Parker, J.C., 2006. Modeling of fluid transport through barriers (Chapter 2). Barrier systems for environmental contaminant containment and treatment, C.C. Chien, H.I. Inyang, and L.G. Everett, (Eds.), CRC Press, Taylor and Francis Group, LLC, Boca Raton, FL, 71-141.
Smith, J.A., Jaffe, P.R., 1994. Benzene transport through landfill liners containing organophilic bentonite. J. Environ. Engrg. 120 (6), 1559–1577.
Spooner, P., 1984. Slurry trench construction for pollution migration control. EPA-540/2-84-001. U.S. Environmental Protection Agency, Cincinnati, Ohio.
Srinivasan, P., Mercer, J.W., 1987. Bio1D – One-Dimensional Model for Comparison of Biodegradation and Adsorption Processes in Contaminant Transport. GeoTrans, Inc., Sterling, VA. 146 pp.
Terzyk, A.P., Chatlas, J., Gauden, P.A., Rychlicki, G., Kowalczyk, P., 2003. Developing the solution analogue of the Tóth adsorption isotherm equation. J. Colloid Interface Sci. 266 (2), 473–476.
Tóth, J., 1995. Thermodynamical correctness of gas/solid adsorption isotherm equations. J. Colloid Interface Sci. 163 (2), 299–302.
van Genuchten, M.Th., Cleary, R.W., 1982. Movement of solutes in soil: computer-simulated and laboratory results. In: Bolt, G.H. (Ed.), Soil Chemistry B. Physico-Chemical Models. Elsevier, New York, NY, pp. 349–383. Ch. 10.
Weber, W.J., McGinley, P.M., Katz, L.E., 1991. Sorption phenomena in subsurface systems: concepts, models, and effects on contaminant fate and transport. Water Res. 25 (5), 499–528.
Weber, W.J., McGinley, P.M., Katz, L.E., 1992. A distributed reactivity model for sorption by soils and sediments. 1. Conceptual basis and equilibrium assessments. Environ. Sci. Technol. 26 (10), 1955–1962.
Wu, Z., Joo, H., Ahn, I.-S., Haam, S., Kim, J.-H., Lee, K., 2004. Organic dye adsorption on mesoporous hybrid gels. Chem. Engrg. J. 102 (3), 277–282.
Xanthakos, P.P., 1979. Slurry Walls. McGraw Hill, New York, NY.
Zheng, C., Wang, P.P., 1999. MT3DMS: Documentation and User's Guide. Contract Report SERDP-99-1. U.S. Army Engrg. R&D Center, Vicksburg, MS. 220 pp.